

Supporting Information for ”Transient response of Southern Ocean ecosystems during Heinrich stadials”

Himadri Saini^{1,2}, Katrin J. Meissner^{1,2}, Laurie Menviel^{1,3}, Karin Kvale⁴

¹Climate Change Research Centre, University of New South Wales, Sydney, New South Wales, Australia

²The Australian Research Council Centre of Excellence for Climate Extremes, Sydney, New South Wales, Australia

³The Australian Centre for Excellence in Antarctic Science, University of Tasmania, Hobart, Tasmania 7001, Australia

⁴GNS Science, 1 Fairway Drive, Avalon 5010, PO Box 30368, Lower Hutt 5040, NZ

Contents of this file

1. Figures S1 to S10

Introduction

The supplementary figures from S1 to S10 complements the respective detailed description provided in the main article.

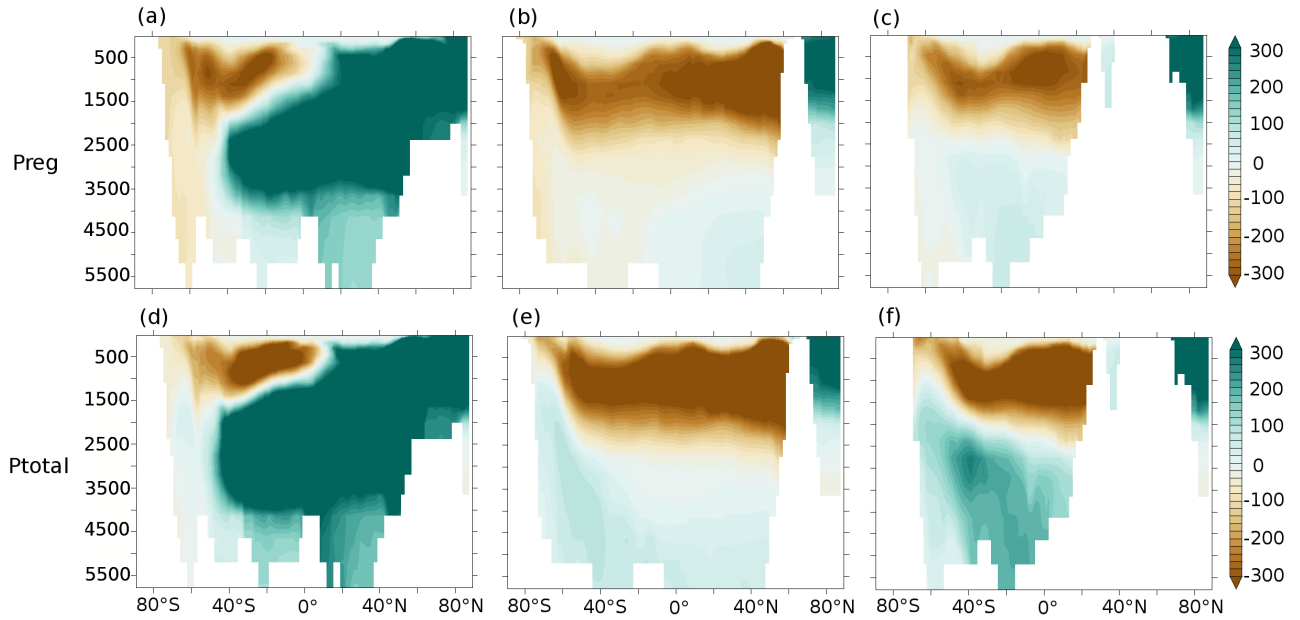


Figure S1. Zonally averaged (top) P_{reg} anomalies ($\mu\text{mol m}^{-3}$) over (left) the Atlantic, (center) the Pacific, and (right) Indian ocean for FW experiment at year 1000 (end of phase 2) compared to the 40ka-control simulation.. Bottom: Same as top for total phosphate (P_{total} , $\mu\text{mol m}^{-3}$) anomalies.

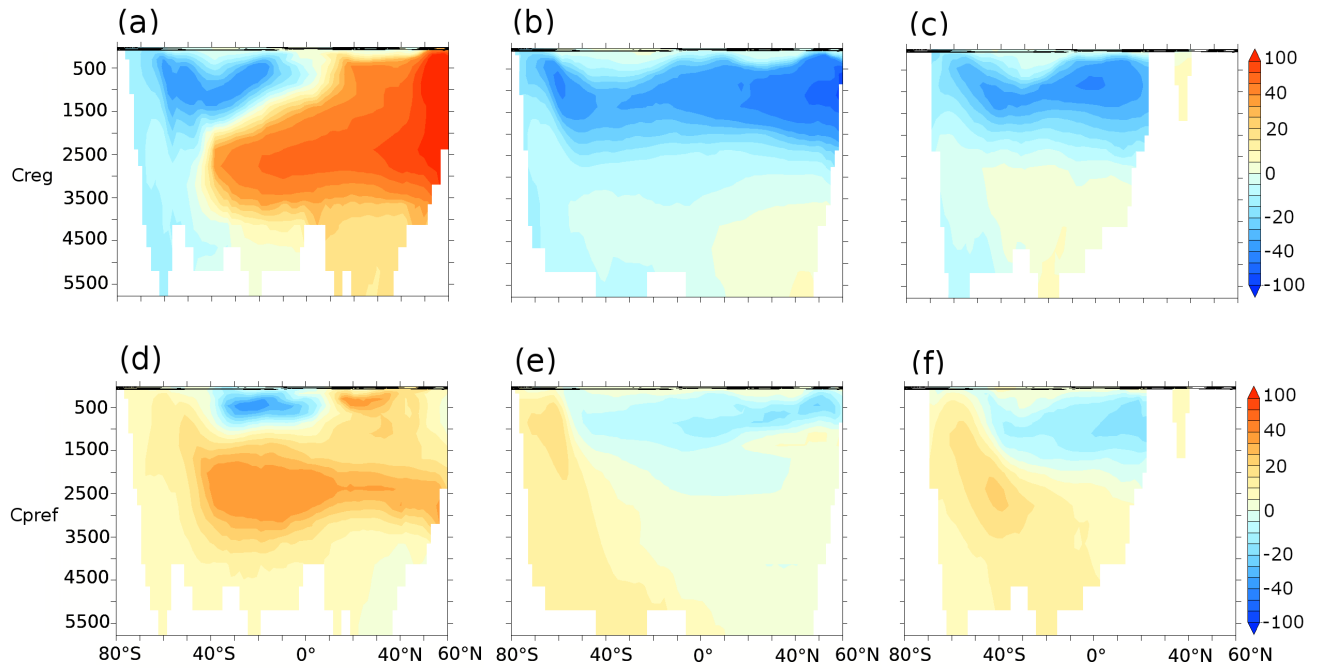


Figure S2. Zonally averaged (top) C_{reg} anomalies (mmol m⁻³) over (left) the Atlantic, (center) the Pacific, and (right) Indian ocean for FW experiment at year 1000 (end of phase 2) compared to the 40ka-control simulation. Bottom: Same as top for C_{pref} (mmol m⁻³) anomalies.

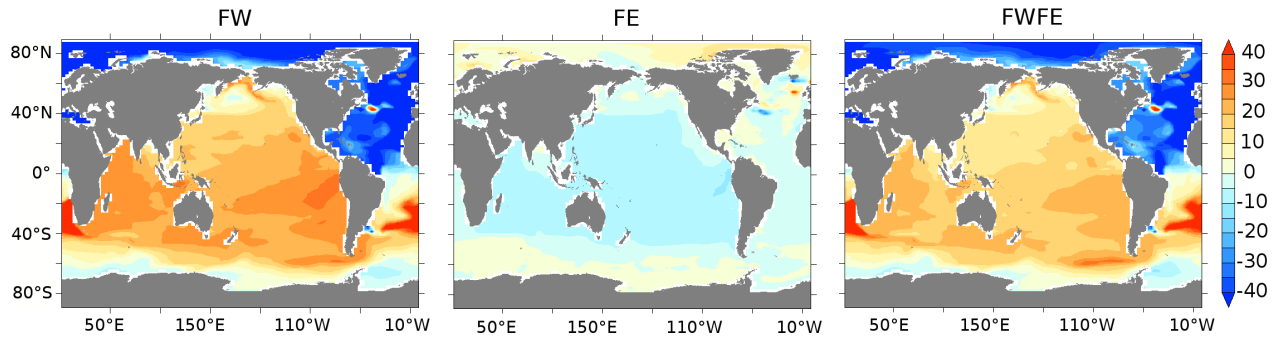


Figure S3. Surface alkalinity anomalies (mmol m⁻³) for experiment (left) FW, (centre) FE, and (right) FWFE at year 1000 (end of phase 2) compared to the 40ka-control simulation.

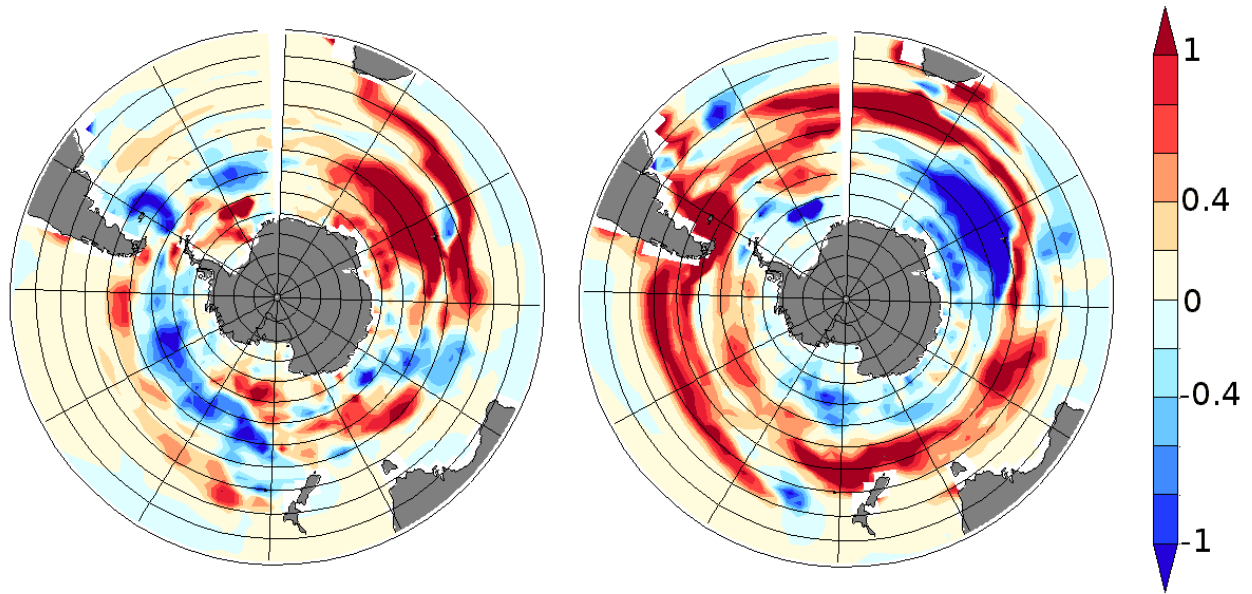


Figure S4. Depth integrated (left) diatom and (right) coccolithophore anomalies (gC m^{-2}) for FW experiment at year 1500 (end of phase 3) compared to FW at year 1000 (end of phase 2).

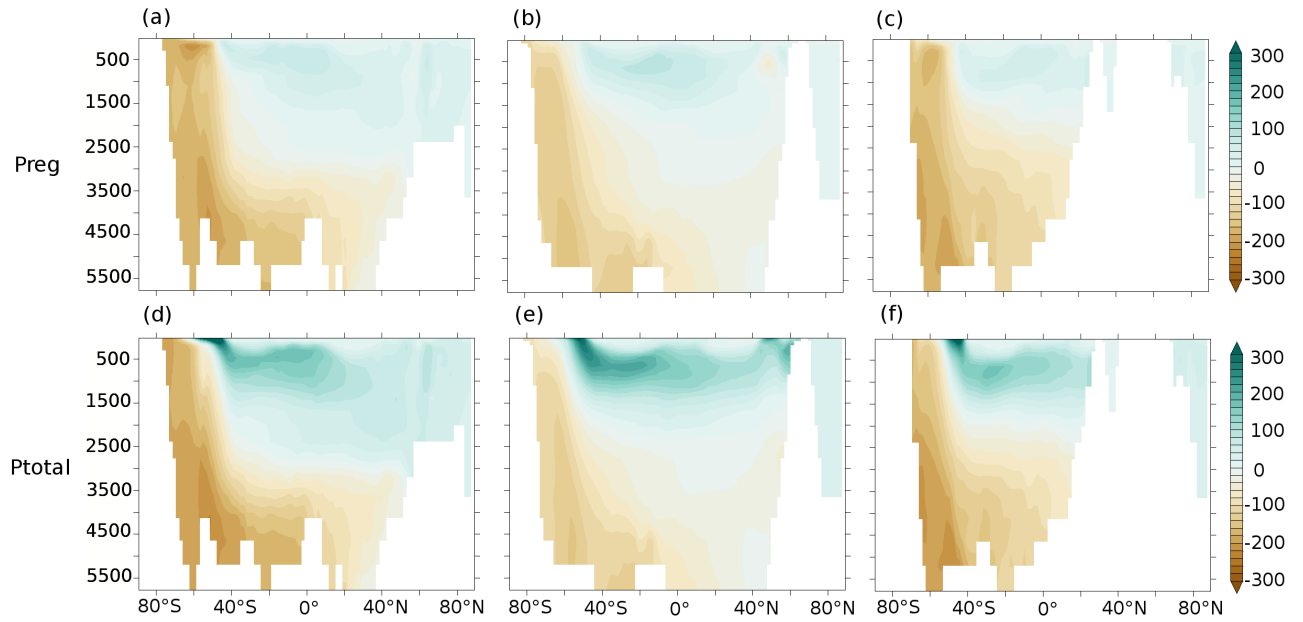


Figure S5. Zonally averaged (top) P_{reg} anomalies ($\mu\text{mol m}^{-3}$) over (left) the Atlantic, (center) the Pacific, and (right) Indian ocean for FE experiment at year 1000 (end of phase 2) compared to the 40ka-control simulation. Bottom: Same as top for total phosphate (P_{total} , $\mu\text{mol m}^{-3}$) anomalies.

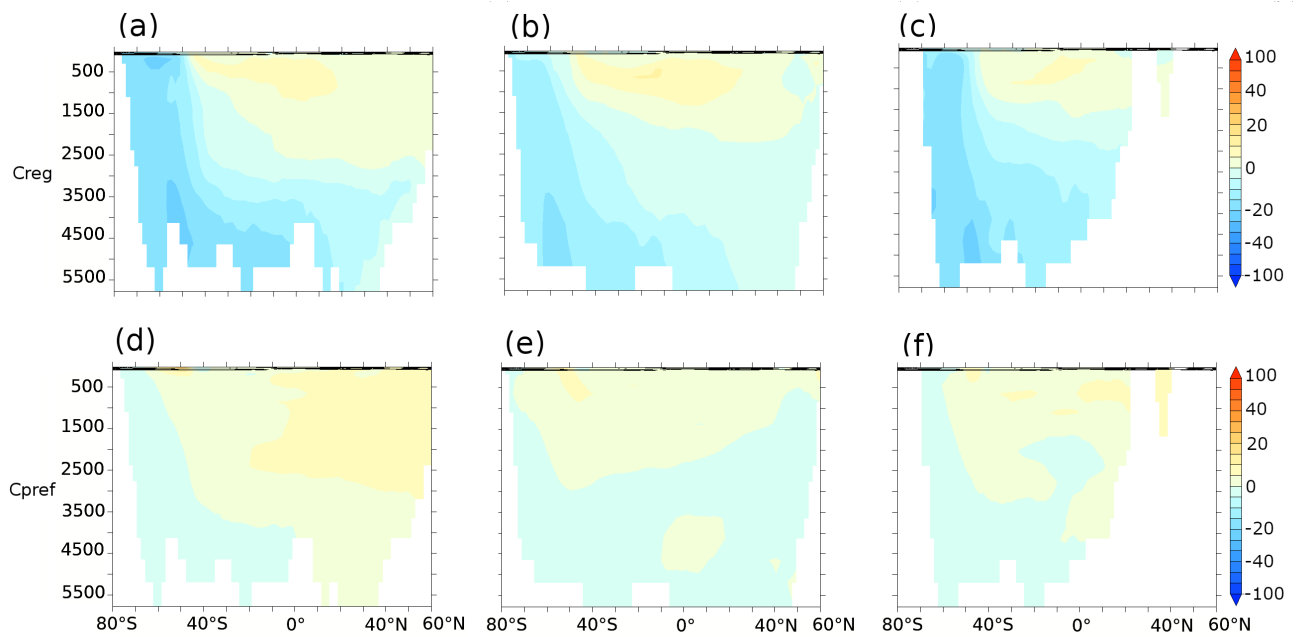


Figure S6. Zonally averaged (top) C_{reg} (mmol m^{-3}) anomalies over (left) the Atlantic, (center) the Pacific, and (right) Indian ocean for FE experiment at year 1000 (end of phase 2) compared to the 40ka-control simulation. Bottom: Same as top for C_{pref} (mmol m^{-3}) anomalies.

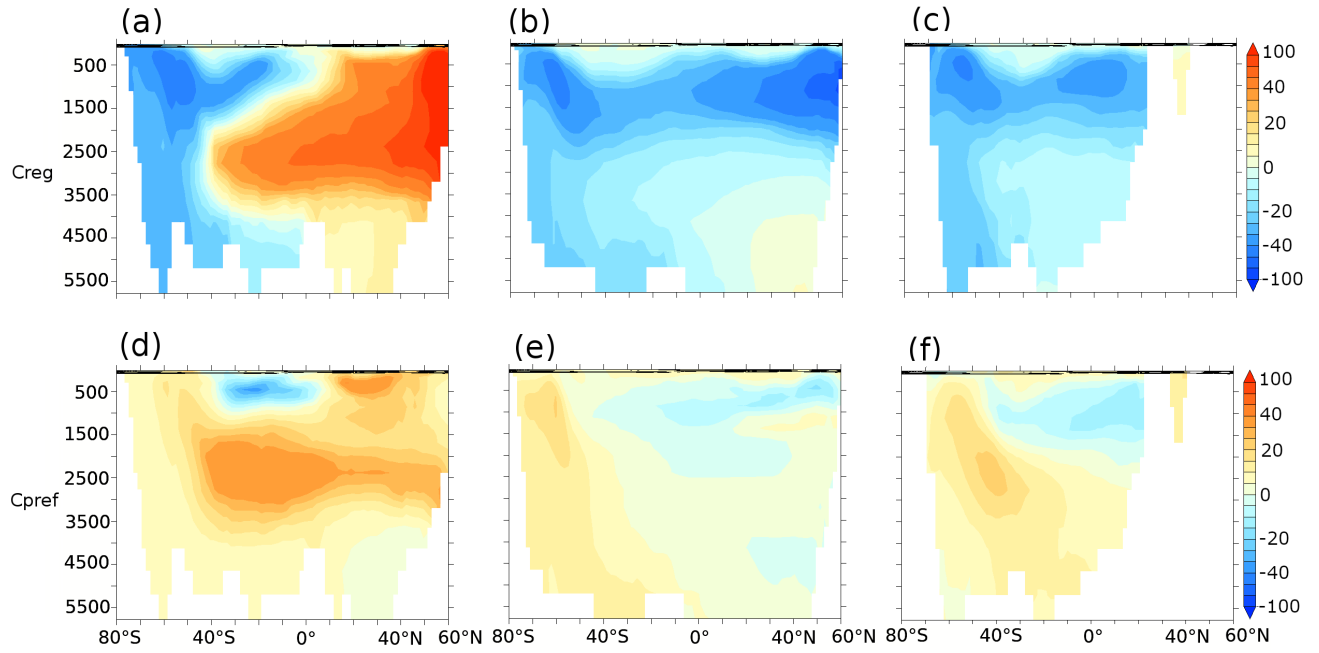


Figure S7. Zonally averaged (top) C_{reg} (mmol m^{-3}) anomalies over (left) the Atlantic, (center) the Pacific, and (right) Indian ocean for FWFE experiment at year 1000 (end of phase 2) compared to the 40ka-control simulation. Bottom: Same as top for C_{pref} (mmol m^{-3}) anomalies.

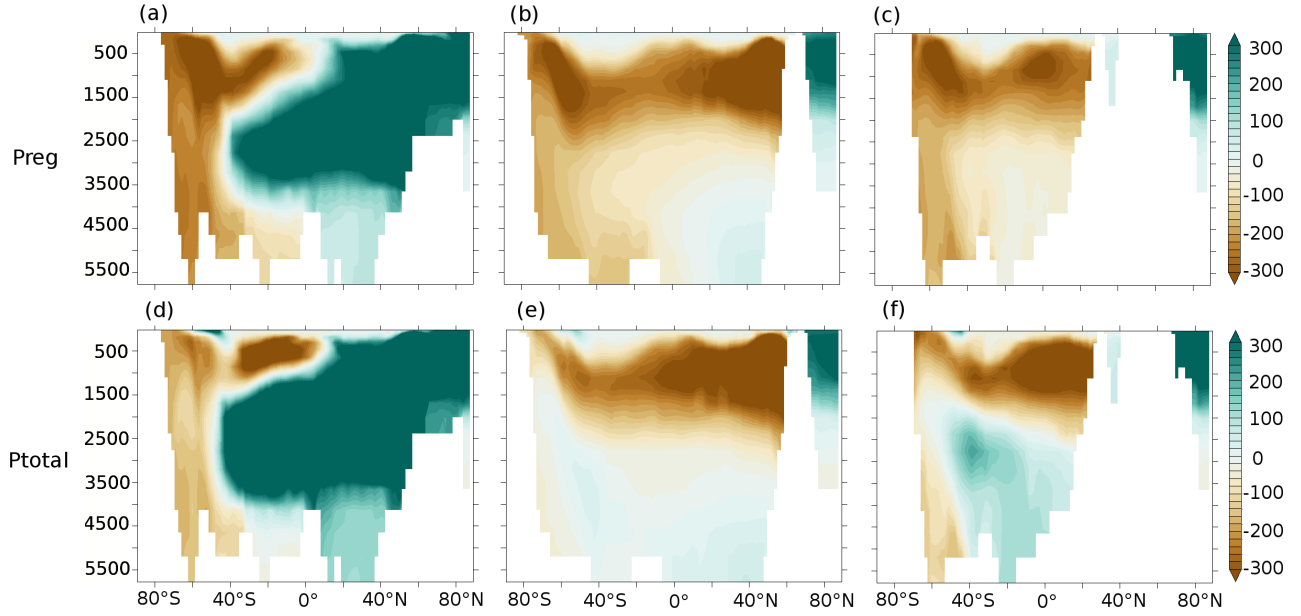


Figure S8. Zonally averaged (top) P_{reg} anomalies ($\mu\text{mol m}^{-3}$) over (left) the Atlantic, (center) the Pacific, and (right) Indian ocean for FWFE experiment at year 1000 (end of phase 2) compared to the 40ka-control simulation. Bottom: Same as top for total phosphate (P_{total} , $\mu\text{mol m}^{-3}$) anomalies.

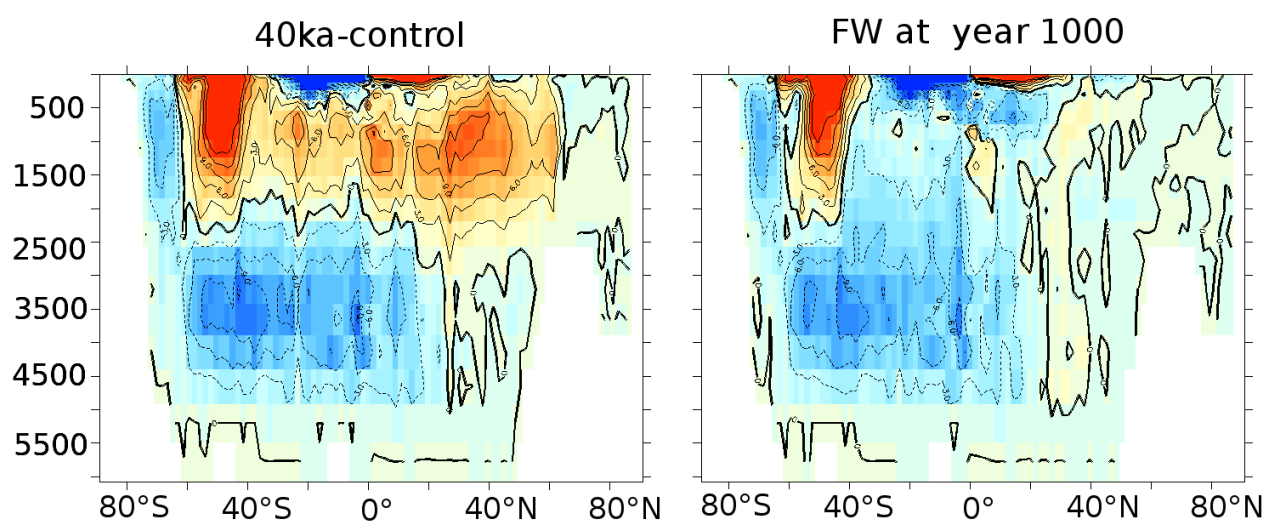


Figure S9. Global overturning streamfunctions (Sv) in experiment (left) 40ka-control and in experiment (right) FW at year 1000 (end of phase 2).

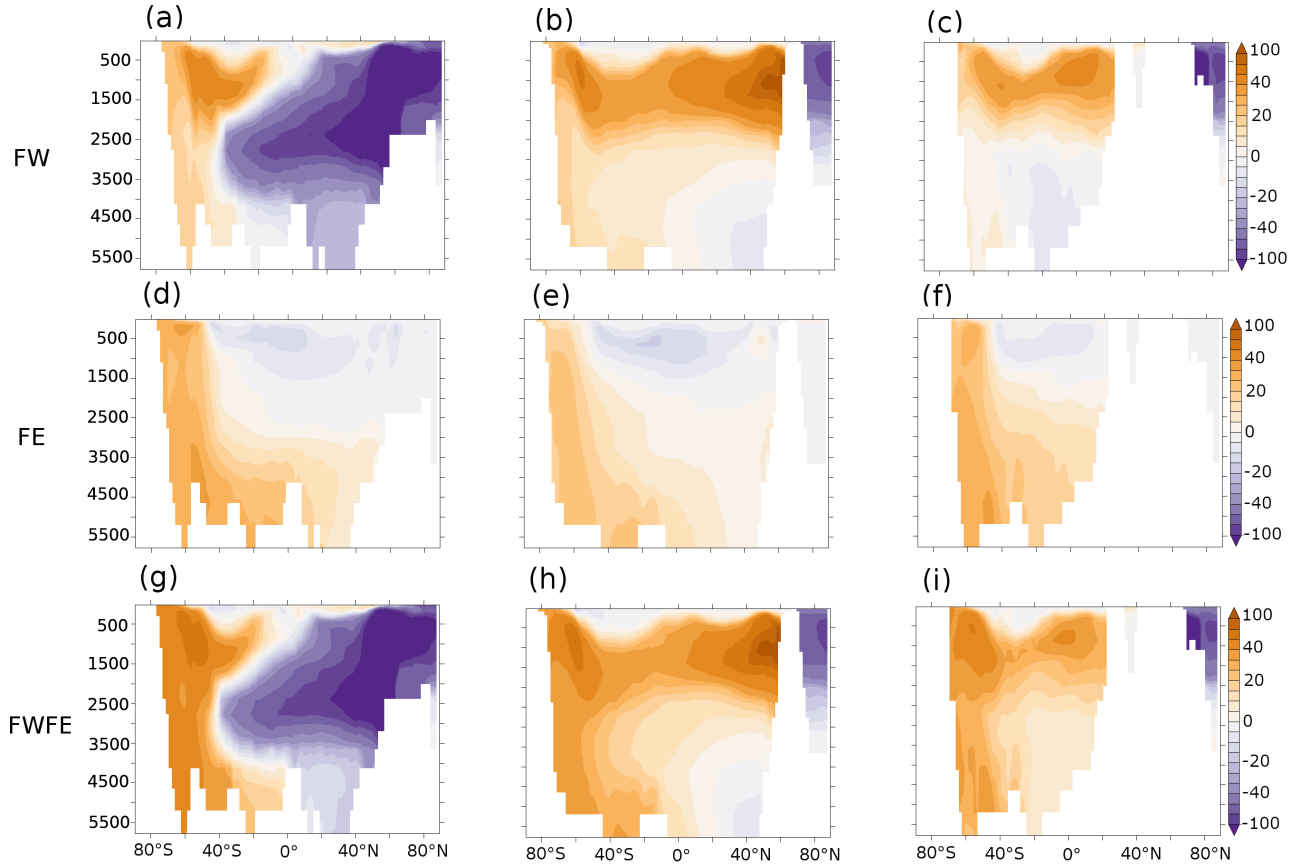


Figure S10. Zonally averaged oxygen anomalies (mmol m⁻³) over (left) the Atlantic, (center) the Pacific, and (right) Indian ocean for experiments (top) FW, (center) FE, and (bottom) FWFE at year 1000 (end of phase 2) compared to the 40ka-control simulation.